The Impact of RF Front-End Characteristics on the Spectral Regrowth of Communications Signals

Kevin G. Gard, *Member, IEEE*, Lawrence E. Larson, *Fellow, IEEE*, and Michael B. Steer, *Fellow, IEEE*

***Abstract*—The nonlinear characteristic of an RF front-end results in in-band distortion and spectral regrowth of digitally modulated signals with distortion being dependent on the statistical variation of the signal. In this paper, the interaction of the nonlinear response with the signal is explored using a time-averaged autocorrelation analysis applied to several limiter-amplifier models having characteristics ranging from soft-to-hard amplitude limiting. The analysis is verified by comparing measured and predicted adjacent channel power rejection for a code-division multiple-access amplifier.**

***Index Terms*—Adjacent channel interference, adjacent channel power ratio (ACPR), autocorrelation function, bandpass nonlinearity, behavioral models, cellular radio, code-division multiple-access (CDMA) signal, code division multiple access, complex Gaussian process, correlation, correlation theory, digital radio, digital radio system, digital signals, digitally modulated carrier, Gaussian processes, limiting amplifier, limiting-amplifier model, microwave amplifiers, modulation, nonlinear amplifier, nonlinear distortion, nonlinear transformation, quadrature input signal, RF envelope model, spectral analysis, spectral regrowth, statistical analysis.**

I. Introduction

DISTORTION of digitally modulated communication front-end circuits is dependent on the amplitude variation characteristics of the input signal and the nonlinear input/output characteristics of the circuits. Circuit-dependent distortion is investigated in this paper by examining several limiting amplifier models with characteristics ranging from soft-to-hard limiting. Hard limiting amplifiers were found to generally produce significantly less distortion than soft limiting amplifiers. However, the distortion characteristics of hard limiters exhibit signal-dependent notches due to partial cancellation between higher and lower order intermodulation-distortion products. The depth of cancellation and input amplitude where distortion cancellation occurs is dependent on the nonlinearity and the amplitude variation characteristics of the input signal.

The impact of amplifier nonlinearity and of signal amplitude characteristics on output distortion are investigated by first developing a time-averaged autocorrelation analysis of the output carrier envelope. This analysis results in a decomposition of the output power spectrum into a summation of distinct spectral components. Each spectral component is in terms of elements of the underlying nonlinear process and of the input signal leading to relationships among the output spectrum, nonlinear model parameters, and characteristics of the input signal. The output spectrum is a summation of spectral terms, each of which is described by a unique combination of coefficients of the nonlinear model and of the Fourier transform of an autocorrelation term of the input signal [1]. Grouping spectral terms yields information on gain-compression/expansion and intermodulation-distortion characteristics, which are not directly observable from the Fourier transform of the output time-domain waveform [2]–[4].

This paper presents a time-averaged autocorrelation analysis of a modulated carrier passed through a wireless nonlinear circuit modeled by a complex power-series behavioral model. Such a model has proven to be adequate for modeling a bandpass nonlinear system with digitally modulated signals [5]. The time-average autocorrelation function of the output complex envelope is formulated, and the output power spectrum is obtained from the Fourier transformation of the autocorrelation function. Spectral regrowth, adjacent channel power ratio (ACPR), and gain-compression analysis results are compared for five limiter amplifier models. Finally, the complex gain characteristic of a code-division multiple-access (CDMA) amplifier is measured and modeled as a complex power series. The model is used to calculate the output power spectrum when a CDMA mobile station and a complex Gaussian input signals are applied to the circuit. Measured and predicted ACPR results are compared and shown to be in excellent agreement.

II. Bandpass Nonlinearity Modeling

The nonlinear response of a circuit generates distortion terms at harmonics of the carrier. However, only intermodulation-distortion terms centered at the carrier frequency determine adjacent channel interference and signal waveform quality. Here we present an overview of bandpass nonlinearity analysis of a modulated carrier passed through a complex power-series-based behavioral model of a nonlinear wireless circuit. This yields a model for the transfer function (of the first harmonic response) in terms of the complex envelope of the input signal. The analysis is then applied to several analytical limiter models commonly used in modeling communication systems.

A. Bandpass Nonlinearity

A wireless digital communication signal is most commonly generated by a quadrature modulator, as shown in Fig. 1. In-phase and quadrature carrier signals are mixed with two

Manuscript received October 1, 2004; revised January 6, 2005. This work was supported by the Center for Wireless Communications, University of California at San Diego, and by Qualcomm Inc.

K. G. Gard and M. B. Steer are with the Electrical and Computer Engineering Department, North Carolina State University, Raleigh, NC 27695-7914 USA (e-mail: kevin_gard@nscu.edu).

L. E. Larson is with the Center for Wireless Communications, Electrical and Computer Engineering Department, University of California at San Diego, La Jolla, CA 92093 USA.

Digital Object Identifier 10.1109/TMTT.2005.848801

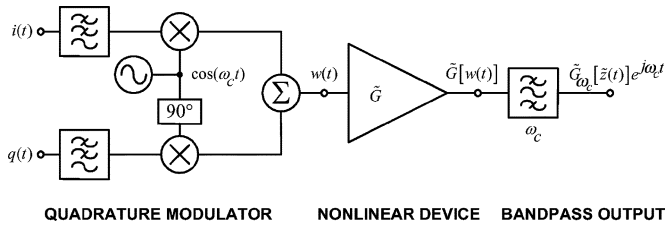

Fig. 1. Block diagram of quadrature modulator and bandpass nonlinearity.

input signals representing the in-phase and quadrature components of the data. The mixed signals are then summed to form the modulated carrier.

This "classic" transmitter front-end architecture is used in most wireless communications applications, and we will now analyze the response of a nonlinear amplifier to the signals it generates. Consider the complex envelope representation of an amplitude and phase modulated carrier $w(t)$ with carrier frequency f_c as follows:

$$w(t) = A(t)\cos\left[\omega_c t + \theta(t)\right] = \frac{1}{2}\tilde{z}(t)e^{j\omega_c t} + \frac{1}{2}\tilde{z}^*(t)e^{-j\omega_c t} \tag{1}$$

where the complex envelope is

$$\tilde{z}(t) = i(t) + jq(t) \tag{2}$$

with $i(t)$ and $q(t)$ being the in-phase and quadrature components of the modulation and $\omega_c = 2\pi f_c$.

The modulated carrier signal is applied to a nonlinear circuit with a gain characteristic $\tilde{G}(v)$ where the AM–AM and AM–PM nonlinearities respond instantly to amplitude changes from the modulated carrier signal [6]. As a result, so-called "memory effects," including thermal time constants, low-frequency biasing effects, and "slow" carrier trapping and de-trapping are ignored. In communication system analysis, the envelope transfer function $\tilde{G}(v)$ is most commonly represented by an analytical model or power-series expansion of a function with amplitude-limiting characteristics.

B. Complex Power-Series Models

A complex power-series expansion can be used to model both the instantaneous AM–AM and AM–PM characteristics

$$\begin{aligned}\tilde{G}\left[w(t)\right] &= \tilde{a}_1 w(t) + \tilde{a}_3 w^3(t) + \tilde{a}_5 w^5(t) + \ldots + \tilde{a}_N w^N(t) \\ &= \sum_{n=0}^{\frac{(N-1)}{2}} \tilde{a}_{2n+1} w^{2n+1}(t).\end{aligned} \tag{3}$$

where $\tilde{a}_1, \tilde{a}_3, \ldots, \tilde{a}_N$ are the complex power-series coefficients. The use of complex coefficients in the power series provides the necessary degrees of freedom to represent both the AM–AM and AM–PM properties of a nonlinear gain characteristic [7]. The complex power-series coefficients are obtained by either a Taylor series expansion of a nonlinear function or a least squared error fit of the series coefficients to a measured, simulated, or derived complex gain characteristic for the device-under-test (DUT). Distortion terms from the model that are centered about the carrier frequency are obtained from a binomial expansion of (3) using (1) as the input

$$w_{\omega_c}^{2n+1}(t) = \left\{\frac{1}{2^{2n}}\binom{2n+1}{n+1}\left[\tilde{z}(t)\right]^{n+1}\left[\tilde{z}^*(t)\right]^n\right\}e^{j\omega_c t}. \tag{4}$$

The output response at the fundamental frequency can also be defined as a function of the complex envelope $\tilde{z}(t)$ [8]

$$\tilde{G}_{\omega_c}\left[w(t)\right] = \tilde{G}_{\omega_c}\left[\tilde{z}(t)\right]e^{j\omega_c t} \tag{5}$$

where

$$\tilde{G}_{\omega_c}\left[\tilde{z}(t)\right] = \sum_{n=0}^{\frac{N-1}{2}} \frac{\tilde{a}_{2n+1}}{2^{2n}}\binom{2n+1}{n+1}\tilde{z}(t)^{n+1}\left[\tilde{z}^*(t)\right]^n. \tag{6}$$

This expression describes the complex envelope of the first harmonic of a modulated carrier signal passed through a bandpass nonlinear circuit described by a complex power series. These coefficients provide a describing function representation of the nonlinearity [9]. We will now use these results to derive the large-signal fundamental response of some well-known nonlinear amplifier models.

C. Limiter Amplifier Models

The hyperbolic tangent function is a convenient function, which is often used for simple modeling of the limiting behavior of amplifiers. It also describes the large-signal low-frequency response of a bipolar transistor differential pair amplifier

$$v_o = L\tanh\left(\frac{g}{L}v_{\text{in}}\right) \tag{7}$$

where g is the linear gain and L is the limit value of the output signal. One drawback of the hyperbolic tangent function is that the "sharpness" of the transition from the linear to the limiting characteristic of the model is fixed in relation to the gain and cannot be adjusted without introducing additional parameters.

Another popular behavioral limiter model, which permits independent control of gain, limiting value, and the sharpness of the transition characteristic is the Cann model [10] given by

$$v_o = \frac{g v_{\text{in}}}{\left[1 + \left(\frac{g}{L}\left|v_{\text{in}}\right|\right)^s\right]^{\frac{1}{s}}} \tag{8}$$

where g is the small-signal gain, L is the limit value of the output signal, and s controls the sharpness of the transition from linear to limiting. One drawback to the Cann limiter model is that it exhibits derivative behavior that leads to nonphysical behavior of the intermodulation products for different values of s [11].

The power-series coefficients for (7) and (8) may be obtained from a Taylor series expansion of each function. However, the range of validity of a Taylor series expansion about a single point is too small to adequately represent an amplifier operating near the gain-compression region. Alternatively, a least squares fit of the power-series coefficients to the limiter response provides a wider range of validity that extends several decibels into the gain-compression region of the limiter response. A least squares fit of odd order 23, 12 coefficients, was applied to each

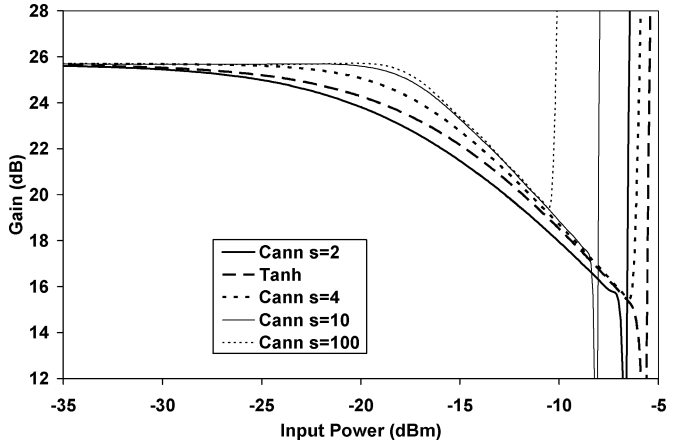

Fig. 2. Carrier gain characteristics of Cann and hyperbolic tangent power-series limiter models.

of the nonlinear carrier transfer functions. An order of 23 was selected as a tradeoff between the range of validity and computational ease. A plot of the carrier gain characteristics from each of the power-series models is shown in Fig. 2. These curves can be used to estimate the gain-compression characteristics and range of model validity for differing s values for the Cann or hyperbolic tangent models.

III. Autocorrelation Analysis of Distortion

We will now use time-averaged autocorrelation analysis to derive expressions for the spectrum of a digitally modulated signal passed through a bandpass nonlinearity. The analysis is performed on several different analytical limiting amplifier models, and the output spectrum and ACPR are calculated as a function of output power.

The output autocorrelation function of the nonlinear model is

$$\tilde{\Re}_{gg}(\tau) = \lim_{T\to\infty} \frac{1}{2T} \int_{-T}^{T} \tilde{G}_{\omega_c}\left[\tilde{z}(t)\right] \tilde{G}^{*}_{\omega_c}\left[\tilde{z}(t+\tau)\right] dt \tag{9}$$

where, from (6),

$$\begin{aligned}\tilde{G}_{\omega_c}\left[\tilde{z}(t)\right]&\tilde{G}^{*}_{\omega_c}\left[\tilde{z}(t+\tau)\right] \\ &= \sum_{n=0}^{\frac{N-1}{2}} \sum_{m=0}^{\frac{N-1}{2}} \frac{\tilde{a}_{2n+1}\tilde{a}^{*}_{2m+1}}{2^{2(n+m)}} \\ &\quad \times \binom{2n+1}{n+1}\binom{2m+1}{m+1} \tilde{z}_1^{n+1} \left(\tilde{z}_1^{*}\right)^{n} \left(\tilde{z}_2^{*}\right)^{m+1} \tilde{z}_2^{m}, \\ &\quad \tilde{z}_1 = \tilde{z}(t); \quad \tilde{z}_2 = \tilde{z}(t+\tau). \end{aligned} \tag{10}$$

Expanding (9) by substituting (10) leads to the output autocorrelation function

$$\begin{aligned}\tilde{\Re}_{gg}(\tau) = &\sum_{n=0}^{\frac{N-1}{2}} \sum_{m=0}^{\frac{N-1}{2}} \frac{\tilde{a}_{2n+1}\tilde{a}^{*}_{2m+1}}{2^{2(n+m)}} \\ &\times \binom{2n+1}{n+1}\binom{2m+1}{m+1} \tilde{\Re}_{z_{2n+1}z_{2m+1}}(\tau) \end{aligned} \tag{11}$$

where

$$\tilde{\Re}_{z_{2n+1}z_{2m+1}}(\tau) = \lim_{T\to\infty} \frac{1}{2T} \int_{-T}^{T} \tilde{z}_1^{n+1} \left(\tilde{z}_1^{*}\right)^{n} \tilde{z}_2^{m} \left(\tilde{z}_2^{*}\right)^{m+1} dt. \tag{12}$$

The output power spectrum is obtained from the Fourier transform of the output autocorrelation function

$$\begin{aligned}\tilde{S}_{gg}(\tau) = &\sum_{n=0}^{\frac{N-1}{2}} \sum_{m=0}^{\frac{N-1}{2}} \frac{\tilde{a}_{2n+1}\tilde{a}^{*}_{2m+1}}{2^{2(n+m)}} \\ &\times \binom{2n+1}{n+1}\binom{2m+1}{m+1} \tilde{S}_{(2n+1)(2m+1)}(f) \end{aligned} \tag{13}$$

where

$$\tilde{S}_{(2n+1)(2m+1)}(f) = \int_{-\infty}^{\infty} \Re_{z_{2n+1}z_{2m+1}}(\tau) e^{-j\omega\tau} d\tau.$$

In general, there are $[(N-1)/2]^2$ autocorrelation and spectral terms in the expansion for an N^{th} odd order power-series expansion. For a particular modulation input signal, the individual autocorrelation and spectrum terms are computed only once and stored in a file. At run time, the spectral components are read, then scaled by the power-series coefficients and input power level, and summed to yield the output spectrum.

The output spectrum terms can be separated into distinct groups describing different nonlinear effects. For instance, the spectral terms correlated to the input signal represent the gain expansion or compression of the desired signal at the output, while all other terms represent the uncorrelated nonlinear distortion about the carrier. The gain compression or expansion terms from (13) are

$$\begin{aligned}\tilde{S}_{gg_{\mathrm{Gain}}}(f) = &\left|\tilde{a}_1\right|^2 \tilde{S}_{11}(f) + \sum_{n=1}^{\frac{N-1}{2}} \frac{1}{2^{2(n+1)}} \binom{2n+1}{n+1} \\ &\times \left[\tilde{a}_1\tilde{a}^{*}_{2n+1}\tilde{S}_{1(2n+1)}(f) + \tilde{a}_{2n+1}\tilde{a}^{*}_{1}\tilde{S}_{(2n+1)1}(f)\right] \end{aligned} \tag{14}$$

while the nonlinear distortion terms from (13) representing the spectral regrowth are

$$\begin{aligned}\tilde{S}_{gg_{\mathrm{Distortion}}}(f) = &\sum_{n=1}^{\frac{N-1}{2}} \sum_{m=1}^{\frac{N-1}{2}} \frac{\tilde{a}_{2n+1}\tilde{a}^{*}_{2m+1}}{2^{2(n+m)}} \\ &\times \binom{2n+1}{n+1}\binom{2m+1}{m+1} \tilde{S}_{(2n+1)(2m+1)}(f). \end{aligned} \tag{15}$$

IV. Spectral Results

Spectral analysis of the limiter models requires evaluation of (13) using the least squares fitted power-series model for each limiter and the $[(N-1)/2]^2$ precomputed spectral terms. The spectral terms are computed by evaluating the $[(N-1)/2]^2$ autocorrelation terms using discrete estimates of (11) from a

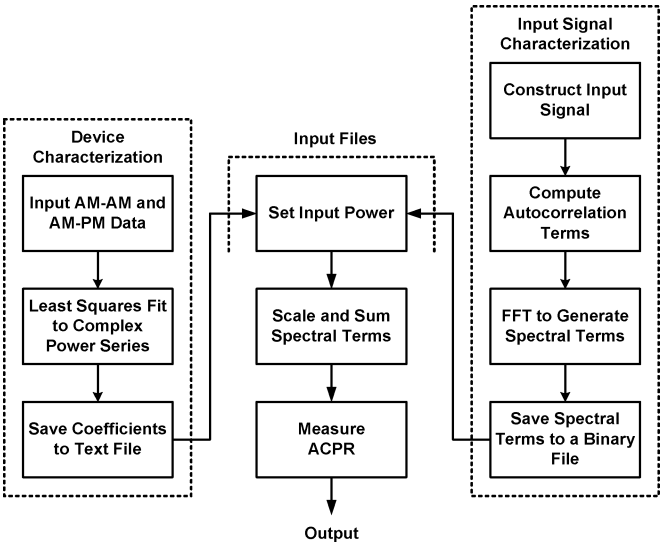

Fig. 3. Flowchart for power-spectrum calculation.

time-domain realization of the input signal [8], then taking the fast Fourier transform (FFT) of each correlation term, and finally saving all the spectral terms in a single file. The power of the input signal used to generate the spectral file is normalized to a convenient value, in this case, 0 dBm or 1 mW, such that the power of each spectral term is simply scaled by the ratio of the desired input power to the normalized input power raised to the appropriate power of the spectral term

$$\tilde{S}_{(2n+1)(2m+1)} = \left(\frac{p_{\text{in}}}{p_{\text{norm}}}\right)^{2(n+m+1)} \tilde{S}_{\text{norm}_{(2n+1)(2m+1)}} \tag{16}$$

where the subscript norm denotes the normalized input power of the spectral term. The output spectrum is calculated by summing the product of the scaled spectral terms from (16) by the corresponding power-series coefficient $\tilde{a}_{2n+1}\tilde{a}^*_{2m+1}$. A flowchart of the spectral calculation is shown in Fig. 3. A sweep of the input power is easily performed by sweeping p_{in} over the power range of interest and recalculating the sum of spectral terms.

A. Spectral Analysis

These results can be used to efficiently calculate the output spectrum of a nonlinear system once the autocorrelation of the input signal and the nonlinear power-series coefficients are determined. An example plot of the composite, gain compression/expansion, and distortion power spectrums for the hyperbolic tangent limiter model are shown in Fig. 4. The power spectrum for the gain-compression/expansion terms from (14) is nearly identical to the spectrum of the input signal. The out-of-band spectrum of the composite signal is limited to approximately 70 dBc by the finite rejection of the CDMA baseband finite impulse response (FIR) filter, as indicated in the plot, where the composite and gain-compression/expansion spectrums converge around ± 3 MHz. However, the distortion spectrum, from (15), clearly shows the distortion that lies underneath the finite rejection of the input signal baseband filter.

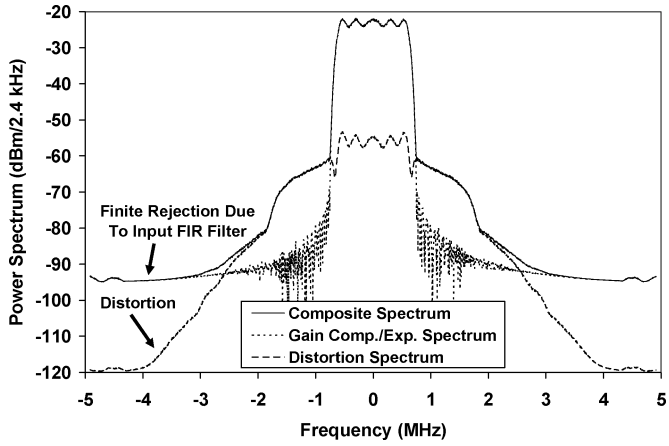

Fig. 4. Spectrum components from autocorrelation analysis.

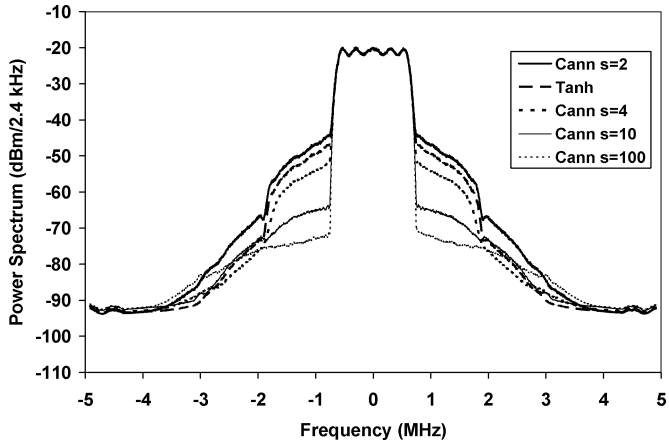

Fig. 5. Total output power spectrum at 6 dBm for each limiter model.

The distortion spectrum also reveals the in-band distortion, which is normally "hidden" by the desired signal when viewing the composite power spectrum. In-band distortion is important for determining signal waveform quality factor ρ degradation [12] in nonlinear amplifiers.

A composite plot of the output power spectrum for each of the limiter models described in Section III, with a CDMA IS-95 reverse link input signal and an output power of 6 dBm, is shown in Fig. 5. For equal output power, the out-of-band distortion is highest for the softer limiter models like the Cann $s = 2$ and hyperbolic tangent models, and lowest for models with a sharper nonlinear transition. These curves can be very useful in predicting CDMA ACPR and waveform quality factor for an amplifier whose gain has been approximated by a Cann or hyperbolic tangent model.

B. Power-Sweep Analysis

Power-sweep characterization of ACPR is important for understanding the nonlinear behavior of a transmitter circuit. Typically, much of the design effort is spent optimizing ACPR performance at the maximum output power specification in an effort to maximize efficiency, while meeting the ACPR specification limits. An input power sweep was performed from -50 to -5 dBm in 0.5-dB steps to obtain an ACPR

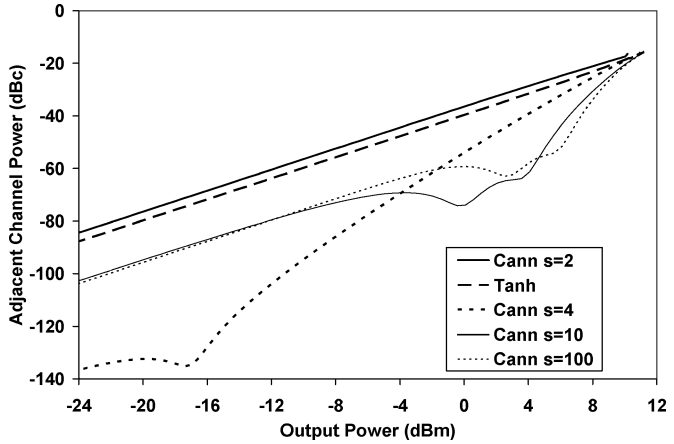

Fig. 6. Adjacent channel power at 885-kHz offset for limiter models.

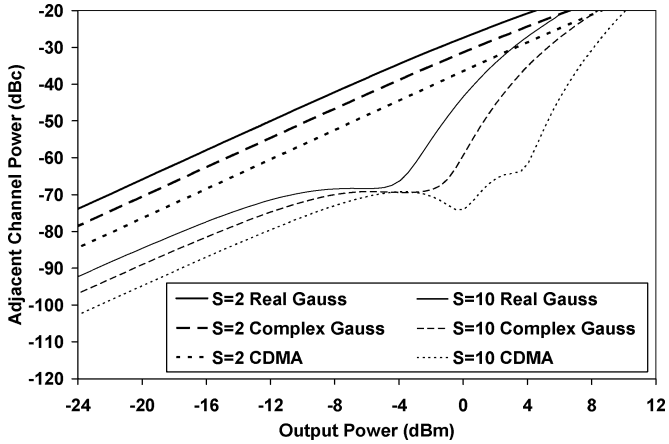

Fig. 7. ACPR for three input signals applied to two limiter models.

as a function of output power for each of the models. The ACPR results are shown in Fig. 6 for a distortion offset of 885 kHz, as defined for the adjacent channel measurement in the IS-95 CDMA specification [13].

There are notable differences in the ACPR produced by the different models. The hyperbolic tangent and Cann $s = 2$ models both exhibit a $2:1$ ACPR slope, which is expected for most class-A or class-AB amplifiers where the third-order term dominates the distortion. However, the Cann $s = 4, 10$, and 100 models exhibit steeper slope at high output power, indicating higher order nonlinear terms dominating the distortion characteristic. Notches in the ACPR response indicate partial cancellation between nonlinear terms. The location of the notch is dependent on the sharpness of the limiter function. Sharper limiter functions provide cancellation at higher output power levels.

Input signal amplitude characteristics also play an important role in determining the intermodulation characteristics. Signals with higher peak-to-average power ratio (PAR) generally require more input power backoff to achieve the same intermodulation-distortion performance as a signal with lower PAR [14]. Three signals with distinctly different amplitude characteristics were used to investigate the signal-dependent intermodulation characteristics of two nonlinear models. The first is a CDMA reverse-link signal with a modest PAR of 5.4 dB. The second is a complex Gaussian signal with a Rayleigh amplitude distribution with a PAR of 11.8 dB. The complex Gaussian signal is an approximate model for orthogonal frequency division multiplexing (OFDM) signals [15] used in wireless local area network (WLAN) systems. The third signal has a real Gaussian amplitude distribution with a PAR of 13.8 dB. ACPR results for each signal applied to the Cann $s = 2$ and 10 models are shown in Fig. 7. Signals with higher amplitude variation yield higher distortion. Notably, the notch locations for the $s = 10$ case occurs at lower input power levels and with a shallower depth for signals with higher amplitude variation.

In summary, it appears that hard limiting results in lower overall adjacent channel power than a soft-limiting front-end. There is an exception in cases where distortion is reduced at lower power levels due to cancellation effects between various distortion components. The effect is signal dependent and is related to amplitude distribution of the input signal. Nevertheless, it is seen that tailoring of the nonlinear response to a particular communication signal will result in reduced adjacent channel distortion at higher input powers.

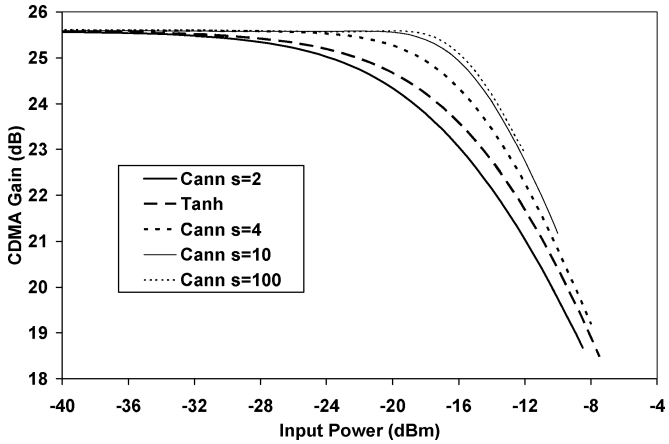

Fig. 8. CDMA gain-compression characteristic.

C. Gain Compression

The gain-compression characteristic of a nonlinearity is also important [16]. The CDMA gain-compression characteristic is measured by comparing the difference in input power and output power for the desired CDMA signal channel. A plot of CDMA gain compression is shown in Fig. 8. The CDMA gain compression is more significant for models with a softer nonlinear transition compared to models with a sharper transition.

Real and complex bandpass Gaussian waveforms have significantly wider amplitude variation than sinusoidal or CDMA waveforms so the gain with these signals should compress at a lower input signal level than a CDMA signal. Similar to the CDMA compression results, the complex Gaussian gain compression is more significant for models with a softer nonlinear transition compared to models with a sharper transition. A comparison of the CDMA input referred $P_{1\,\mathrm{dB}}$ compression point to the sinusoidal compression results for the nonlinear models is shown in Table I. The wider amplitude variations of the

TABLE I
GAIN COMPRESSION FOR DIFFERENT INPUT SIGNALS

Nonlinear Model	Real Gaussian P_{1dB} (dBm)	Complex Gaussian P_{1dB} (dBm)	CDMA P_{1dB} (dBm)	Sinusoidal P_{1dB} (dBm)
Tanh	-22.5	-21.0	-19.5	-19.0
S=2	-24.0	-22.5	-21.0	-20.0
S=4	-20.0	-18.5	-16.5	-16.0
S=10	-18.5	-17.0	-15.0	-14.0
S=100	NA	-17.5	-14.5	-14.0

real Gaussian signal contribute more to the gain compression, resulting in a 3.0–3.5 dB lower input referred compression point compared to a CDMA signal. Interestingly, the complex Gaussian signal has approximately 1.5 dB higher input compression point than the real Gaussian signal. The input $P_{1\,\mathrm{dB}}$ compression points could not be accessed for the Cann $s = 100$ limiter model for the real Gaussian signal because the dynamic range of the power-series fit is not wide enough to accommodate the 13-dB peak-to-average ratio of the input signal at 1-dB gain compression.

V. MEASUREMENTS

The general time-average autocorrelation function and the complex Gaussian moment methods were used to calculate the output power spectrum and ACPR of an integrated RF amplifier with CDMA and complex Gaussian input signals. The DUT is a 835-MHz CDMA driver amplifier device fabricated using a GaAs MESFET technology [17]. The device is a two-stage amplifier designed to provide 23.4 dB of power gain, in a 50-Ω system, and meet CDMA ACPR specification requirements at an output power of 8 dBm. A vector network analyzer, with a built in power-sweep function, was used to measure the AM–AM and AM–PM over an input power range of -25 to -2 dBm. The measured AM–AM and AM–PM characteristics were fit to a complex power series of odd order $N = 23$ using a least squares solution. The resulting complex power-series coefficients are shown in Table II and a plot of the power-series model and measured data are shown in Fig. 9.

A carrier modulated with an IS-95 CDMA reverse-link signal is applied to the amplifier circuit and the output distortion measured using a spectrum analyzer. Specifically, an Agilent ESG series signal generator with the capability to generate an IS-95 CDMA signal was used as the signal source and an Agilent vector signal analyzer (VSA) was used to measure ACPR. The VSA equipment has built-in measurement routines to measure ACPR for specified offsets to the carrier frequency. ACPR is the ratio, in decibels, of the distortion power, in a 30-kHz bandwidth offset by $\pm$885 kHz, and the desired channel power, in a 1.23-MHz bandwidth, as defined in the IS-95 Standard [13]. The measured and calculated ACPR is shown in Fig. 10. The

TABLE II
COMPLEX POWER SERIES COEFFICIENTS FOR 835-MHz CDMA AMPLIFIER

Term	Units	Real Coefficient	Imaginary Coefficient
$\tilde{a}_1$	1	1.47437438509120E+01	2.13403737823950E+00
$\tilde{a}_3$	v^{-2}	-6.70889896661973E+01	-2.06242049102448E+01
$\tilde{a}_5$	v^{-4}	-6.34509397147117E+03	2.64680409468526E+03
$\tilde{a}_7$	v^{-6}	-2.02512977741845E+05	-5.02911140999704E+04
$\tilde{a}_9$	v^{-8}	1.72980263843510E+07	-1.04643833028688E+06
$\tilde{a}_{11}$	v^{-10}	-3.28432949645493E+08	3.76656913802756E+07
$\tilde{a}_{13}$	v^{-12}	1.99599335429889E+09	-2.78828805740329E+08

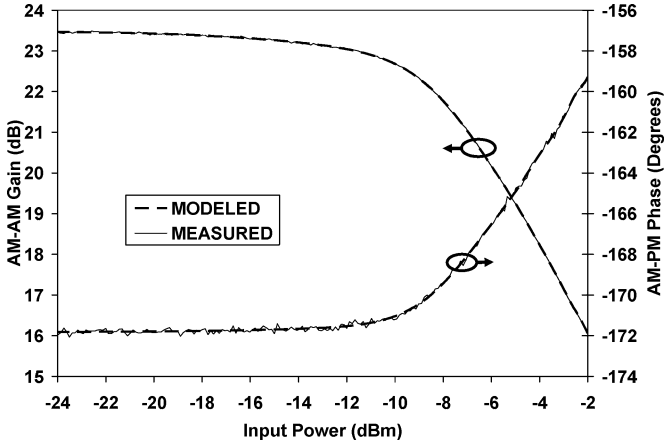

Fig. 9. Modeled and measured AM–AM/AM–PM response for a CDMA amplifier.

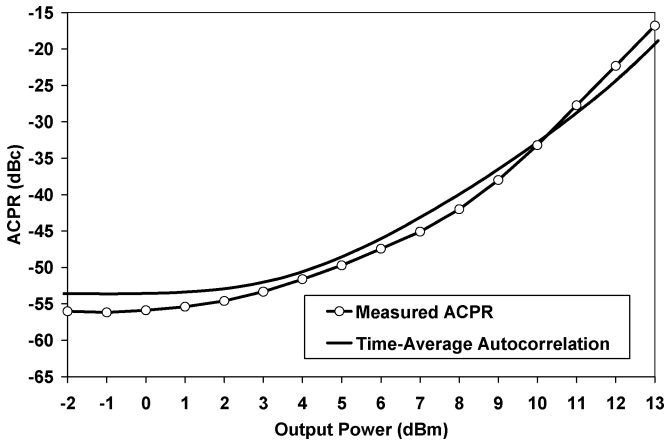

Fig. 10. Measured and calculated ACPR for CDMA reverse-link signal.

ACPR was calculated using the general time-average correlation function formulation for the gain-compression/expansion terms (14), the distortion terms (15), and the power-series coefficients from Table II. The simulated ACPR results using the composite of the gain compression/expansion (14) and distortion terms (15) agree well with the measured data shown Fig. 10. The ACPR plateaus at lower output power because of the finite rejection of the CDMA baseband filter used by the waveform generator.

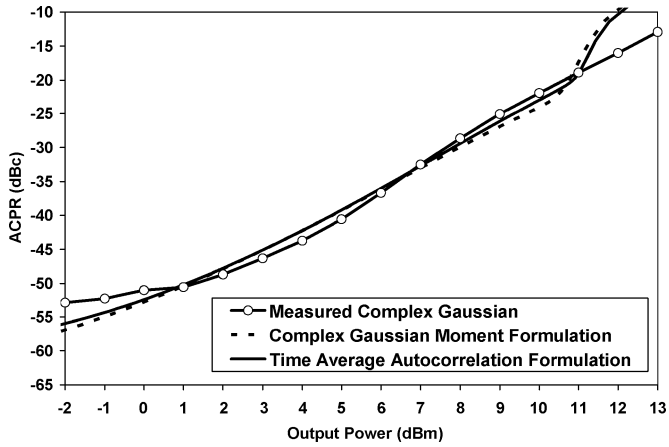

Fig. 11. Measured and calculated ACPR for a complex Gaussian input signal.

A complex Gaussian signal was also used to measure ACPR to compare against both the complex Gaussian moment [8] and the time-average autocorrelation formulations. The ACPR measurements along with the predicted ACPR from both the complex Gaussian moment and time-average autocorrelation formulations are shown in Fig. 11. The measured and predicted ACPR are in good agreement below an output power level of 11 dBm. Both the complex Gaussian moment and time-average autocorrelation formulations deviate from the measured data above 11 dBm because of the limited dynamic range of the complex power-series model of the nonlinear amplifier.

VI. Conclusion

An efficient and accurate method for analyzing the power spectrum of modulated carriers passed through a nonlinear wireless circuit has been presented. The method is based on formulating the time-average autocorrelation function for a signal passed through a complex power-series behavioral model of the AM–AM and AM–PM characteristics of a wireless amplifier. The power spectrum of the signal is obtained via the Fourier transformation of the output autocorrelation function leading to a summation of $[(N-1)/2]^2$ terms for an Nth odd-order power-series expansion of the nonlinearity. Autocorrelation analysis was applied to limiter amplifier models leading to insight into the distortion process. The analysis was validated by comparing ACPR results from the model with measured data from a CDMA amplifier.

Acknowledgment

The authors wish to thank the reviewers for their many helpful suggestions and comments.

References

[1] J. G. Proakis and D. G. Manolakis, *Digital Signal Processing: Principles, Algorithms, and Applications*, 2nd ed. New York: Macmillan, 1992.

[2] S.-W. Chen, W. Panton, and R. Gilmore, "Effects of nonlinear distortion on CDMA communication systems," *IEEE Trans. Microw. Theory Tech.*, vol. 44, no. 12, pp. 2743–2750, Dec. 1996.

[3] J. S. Kenney and A. Leke, "Power amplifier spectral regrowth for digital cellular and PCS applications," *Microwave J.*, vol. 38, no. 10, p. 74, Oct. 1995.

[4] W. Struble, F. McGrath, I. Harrington, and P. Nagle, "Understanding linearity in wireless communication amplifiers," *IEEE J. Solid-State Circuits*, vol. 32, no. 9, pp. 1310–1318, Sep. 1997.

[5] G. L. Heiter, "Characterization of nonlinearities in microwave devices and systems," *IEEE Trans. Microw. Theory Tech.*, vol. MTT-21, no. Dec., pp. 797–805, 1973.

[6] N. Blachman, "Band-pass nonlinearities," *IEEE Trans. Inf. Theory*, vol. IT-10, no. 2, pp. 162–164, Apr. 1964.

[7] M. B. Steer and P. J. Khan, "An algebraic formula for the output of a system with large-signal, multifrequency excitation," *Proc. IEEE*, vol. 71, no. 1, pp. 177–179, Jan. 1983.

[8] K. Gard, M. B. Steer, and L. E. Larson, "Generalized autocorrelation analysis of spectral regrowth from bandpass nonlinear circuits," in *IEEE MTT-S Int. Microwave Symp. Dig.*, vol. 1, 2001, pp. 9–12.

[9] L. Wadel, "Describing function as power series," *IRE Trans. Autom. Control*, vol. AP-7, no. 4, p. 50, 1962.

[10] A. J. Cann, "Nonlinearity model with variable knee sharpness," *IEEE Trans. Aerosp. Electron. Syst.*, vol. AES-16, pp. 874–877, Nov. 1980.

[11] S. L. Loyka, "On the use of Cann's model for nonlinear behavioral-level simulation," *IEEE Trans. Veh. Technol.*, vol. 49, no. 5, pp. 1982–1985, Sep. 2000.

[12] V. Aparin, "Analysis of CDMA signal spectral regrowth and waveform quality," *IEEE Trans. Microw. Theory Tech.*, vol. 49, no. 12, pp. 2306–2314, Dec. 2001.

[13] *Mobile Station-Base Station Compatibility Standard for Dual-Mode Wide-Band Spread-Spectrum Cellular Systems*, TIA/EIA IS-95, 1993.

[14] J. F. Sevic and M. B. Steer, "On the significance of envelope peak-to-average ratio for estimating the spectral regrowth of an RF/microwave power amplifier," *IEEE Trans. Microw. Theory Tech.*, vol. 48, no. 6, pp. 1068–1071, Jun. 2000.

[15] P. Banelli and S. Cacopardi, "Theoretical analysis and performance of OFDM signals in nonlinear AWGN channels," *IEEE Trans. Commun.*, vol. 48, no. 3, pp. 430–441, Mar. 2000.

[16] H. Gutierrez, K. Gard, and M. B. Steer, "Nonlinear gain compression in microwave amplifiers using generalized power-series analysis and transformation of input statistics," *IEEE Trans. Microw. Theory Tech.*, vol. 48, no. 10, pp. 1774–1777, Oct. 2000.

[17] V. Aparin, K. Gard, G. Klemens, and C. Persico, "GaAs RFIC's for CDMA/AMPS dual-band wireless transmitters," in *IEEE MTT-S Int. Microwave Symp. Dig.*, vol. 1, 1998, pp. 81–84.

Kevin G. Gard (S'92–M'95) received the B.S. and M.S. degrees in electrical engineering from North Carolina State University, Raleigh, in 1994 and 1995, respectively, and the Ph.D. degree in electrical engineering from the University of California at San Diego, La Jolla, in 2003.

He is currently the William J. Pratt Assistant Professor with the Electrical and Computer Engineering Department at North Carolina State University. From 1996 to 2003, he was with Qualcomm Inc., San Diego, CA, where he was a Staff Engineer and Manager responsible for the design and development of RF integrated circuits (RFICs) for CDMA wireless products. He has designed SiGe BiCMOS, Si BiCMOS, and GaAs metal–semiconductor field-effect transistor (MESFET) integrated circuits for cellular and personal communication systems (PCS) CDMA, wide-band code division multiple access (WCDMA), and AMPS transmitter applications. His research interests are in the areas of integrated circuit design for wireless applications and analysis of nonlinear microwave circuits with digitally modulated signals.

Dr. Gard is a member of the IEEE Microwave Theory and Techniques Society (IEEE MTT-S), the IEEE Solid-State Circuits Society, Eta Kappa Nu, and Tau Beta Pi.

Lawrence E. Larson (S'82–M'86–SM'90–F'00) received the B.S. and M.Eng. degrees in electrical engineering from Cornell University, Ithaca, NY, in 1979 and 1980, respectively, and the Ph.D. degree in electrical engineering from the University of California at Los Angeles (UCLA), in 1986.

From 1980 to 1996, he was with Hughes Research Laboratories, Malibu, CA, where he directed the development of high-frequency microelectronics in GaAs, InP, Si/SiGe, and microelectromechanical systems (MEMS) technologies. In 1996, he joined the faculty of the University of California at San Diego (UCSD), La Jolla, where he is currently the Inaugural Holder of the Communications Industry Chair. He is currently Director of the Center for Wireless Communications, UCSD. During the 2000–2001 academic year, he was on leave with IBM Research, San Diego, CA, where he directed the development of RF integrated circuits (RFICs) for third-generation (3G) applications. He has authored or coauthored over 200 papers. He holds 27 U.S. patents.

Dr. Larson was the recipient of the 1995 Hughes Electronics Sector Patent Award for his research on RF MEMS technology. He was corecipient of the 1996 Lawrence A. Hyland Patent Award of Hughes Electronics for his research on low-noise millimeter-wave high electron-mobility transistors (HEMTs), and the 1999 IBM Microelectronics Excellence Award for his research in Si/SiGe HBT technology.

Michael B. Steer (S'76–M'82–SM'90–F'99) received the B.E. and Ph.D. degrees in electrical engineering from the University of Queensland, Brisbane, Australia, in 1976 and 1983, respectively.

He is currently a Professor with the Department of Electrical and Computer Engineering, North Carolina State University, Raleigh. In 1999 and 2000, he was a Professor with the School of Electronic and Electrical Engineering, The University of Leeds, where he held the Chair in microwave and millimeter-wave electronics. He was also Director of the Institute of Microwaves and Photonics, The University of Leeds. He has authored approximately 300 publications on topics related to RF, microwave and millimeter-wave systems, high-speed digital design, and RF and microwave design methodology and circuit simulation. He coauthored *Foundations of Interconnect and Microstrip Design* (New York: Wiley, 2000).

Prof. Steer is active in the IEEE Microwave Theory and Techniques Society (IEEE MTT-S). In 1997, he was secretary of the IEEE MTT-S. From 1998 to 2000, he was an elected member of its Administrative Committee. He is the Editor-in-Chief of the IEEE TRANSACTIONS ON MICROWAVE THEORY AND TECHNIQUES (2003–2006). He was a 1987 Presidential Young Investigator (USA). In 1994 and 1996, he was the recipient of the Bronze Medallion presented by the Army Research Office for "Outstanding Scientific Accomplishment." He was also the recipient of the 2003 Alcoa Foundation Distinguished Research Award presented by North Carolina State University.